

Steam activation of biochars facilitates kinetics and pH-resilience of sulfamethazine sorption

Anushka Upamali Rajapaksha^{1,2} · Meththika Vithanage² · Sang Soo Lee¹ · Dong-Cheol Seo³ · Daniel C. W. Tsang⁴ · Yong Sik Ok^{1,4}

Received: 26 September 2015 / Accepted: 27 November 2015 / Published online: 7 December 2015
© Springer-Verlag Berlin Heidelberg 2015

Abstract

Purpose Sulfamethazine (SMT) is increasingly detected in environmental matrices due to its versatile use as antibiotics. We aimed to investigate the benefits and roles of steam activation of biochars with respect to SMT sorption kinetics and equilibrium sorption.

Materials and methods Biochars were produced from burcucumber plant and tea waste using a pyrolyzer at a temperature of 700 °C for 2 h. The biochar samples were treated with 5 mL min⁻¹ of steam for an additional 45 min for post-synthesis steam activation. The SMT sorption on the unmodified and steam activated biochars were compared.

Results and discussion The time taken to reach equilibrium was significantly less for steam activated biochars (~4 h) than non-activated biochars (>24 h). Up to 98 % of SMT could be removed from aqueous solutions by steam activated biochars. The sorption kinetic behaviors were well described by the pseudo-second model and SMT sorption rates of steam activated biochars ($k_2 \sim 1.11\text{--}1.57 \text{ mg g}^{-1} \text{ min}^{-1}$) were

significantly higher than that of the unmodified biochars ($k_2 \sim 0.04\text{--}0.11 \text{ mg g}^{-1} \text{ min}^{-1}$) because of increased availability of accessible porous structure with averagely larger pore diameters. Moreover, the equilibrium sorption on the unmodified biochars was significantly influenced by increasing solution pH (~30–50 % reduction) because of speciation change of SMT, whereas steam activated biochars manifested much stronger sorption resilience against pH variation (~2–4 % reduction only) because the enhanced porosity offset the effect of unfavorable electrostatic repulsion.

Conclusions The observed features of steam activated biochars would render their applications more versatile and reliable in field throughout changeable environmental conditions.

Keywords Antibiotics · Charcoal · Designer biochar · Engineered biochar · Sorption kinetics

1 Introduction

Veterinary pharmaceuticals including antibiotics, antiparasitics, and anti-inflammatory medicines are produced in large quantities and widely applied all over the world (Thiele-Bruhn 2003; Boxall et al. 2004). These antibiotics are deployed to support the health and growth of animals; however, widespread detection of residual antibiotics in the environment has been reported, causing land contamination and posing health risk to non-target animal species and human receptors (Margalida et al. 2014; Ok et al. 2011). The commonly encountered contamination pathways are through manufacturing process of antibiotics, treatment of animals, and disposal of carcasses, urine, feces, and unused products (Kim et al. 2011; Margalida et al. 2014). Sulfamethazine (SMT) is commonly used in swine and cattle livestock industry to control diseases as well as in livestock feeds. Recent investigations have

Responsible editor: Hailong Wang

✉ Daniel C. W. Tsang
dan.tsang@polyu.edu.hk

✉ Yong Sik Ok
soilok@kangwon.ac.kr

¹ Korea Biochar Research Center, Kangwon National University, Chuncheon, South Korea

² Chemical and Environmental Systems Modeling Research Group, Institute of Fundamental Studies, Kandy, Sri Lanka

³ Department of Bio-Environmental Sciences, Suncheon National University, Suncheon, South Korea

⁴ Department of Civil and Environmental Engineering, Hong Kong Polytechnic University, Hung Hom, Kowloon, Hong Kong, China

shown frequent detection of SMT in soils and waters. For example, recorded SMT values in swine manure include 0.01–29 mg kg⁻¹ in China, 0–7.2 mg kg⁻¹ in Germany (Hamscher et al. 2002), and 3.3–8.7 mg kg⁻¹ in Switzerland (Haller et al. 2002), respectively. In recent years, outbreaks of foot-and-mouth disease in China and Korea led to the culling of hundreds of thousands of pigs/cattle and burial of massive amounts of carcasses in soil, from which SMT may leach out and arouse significant environmental concerns (Aust et al. 2010; Lim et al. 2014). Considering chemistry of SMT, it is hydrophilic and ionizable antimicrobial chemical consisting of nonpolar core and multiple polar functional groups (amine and sulfonamide groups) (Thiele-Bruhn 2003). These specific properties of SMT make the immobilization of SMT more complex than other non-ionizable organic compounds in the natural environment.

In recent years, biochar has been highlighted as an excellent sorbent to remediate organic and inorganic contamination in soil as well as enhance soil quality and fertility (Ahmad et al. 2014; Tsang and Yip 2014; Rinklebe et al. 2015; Zhang et al. 2015). It can be produced by thermal pyrolysis of organic feedstocks under limited supply of air (Lehmann and Joseph 2009; Mohan et al. 2014). Biochar produced by optimal pyrolysis conditions and suitable modifications displayed promising sorption capacities for both inorganic and organic contaminants (Rajapaksha et al. 2015; Wang et al. 2015). In particular, our previous work indicated that the biochar derived from burcucumber (an invasive plant biomass) and tea waste can effectively immobilize SMT and mitigate its potential leaching in soil (Rajapaksha et al. 2014; Vithanage et al. 2014).

It should be noted that lignocellulosic biomass (e.g., burcucumber) generally requires higher pyrolysis temperatures (600–700 °C) to produce microporous biochar with high surface area (Rajapaksha et al. 2015). Such biochar would possess highly aromatic and well-organized carbon layers, but have fewer hydrogen- and oxygen-containing functional groups due to dehydration and deoxygenation of biomass (Uchimiya et al. 2011; Ahmad et al. 2014). These surface characteristics are good for sorption of hydrophobic organics but show lower ion exchange capacities (Tsang et al. 2007; Liu et al. 2008; Novak et al. 2009), which may limit its applicability for polar and ionizable antibiotics such as SMT. Steam activation process could be employed to modify the biochar after synthesis because this could increase its sorption capacity for SMT by 55 % to approximately 35 mg g⁻¹ (Rajapaksha et al. 2014, 2015). In general, physical modification of biochar by using steam as an oxidizing agent is considered relatively simple and economically feasible in large-scale applications.

The objectives of this study are to evaluate the advantages and roles of steam activated biochars using kinetic parameters and sorption resilience at varying pH as performance

indicators in comparison with those of unmodified biochars produced from lignocellulosic burcucumber and tea waste.

2 Materials and methods

2.1 Biochar production and modification

Biochars were produced from burcucumber plant and tea waste using a pyrolyzer (N11/H Nabertherm, Germany) under a limited supply of air. A pyrolysis temperature of 700 °C was maintained for 2 h. For post-synthesis steam activation, biochar samples were treated with 5 mL min⁻¹ of steam for an additional 45 min. Biochars produced from burcucumber (BBC) and tea waste (TWBC) were designated as BBC-700, BBC-700S, TWBC-700, and TWBC-700S, respectively. The letter “S” represents steam activated biochars. Elemental compositions (C, H, N, S, and O) of biochars were determined by dry combustion, using an elemental analyzer (model EA1110, CE Instruments, Milan, Italy). The moisture, mobile matter, ash, and residual matter contents were determined as described before (Ahmad et al. 2012; Rajapaksha et al. 2015). The pH of biochars was determined in deionized water (1 g/5 mL). Brunauer–Emmett–Teller (BET) specific surface area, total pore volume, and pore diameter were determined using a gas sorption analyzer (NOVA-1200; Quantachrome Corp., Boynton Beach, FL, USA).

2.2 Sorption kinetic experiments

Kinetic studies were conducted at four different pH values of 3, 5, 7, and 9 (i.e., representing natural pH range in soils and waters) under ammonium phosphate and ammonium acetate-buffered conditions, at initial SMT concentrations of 10 mg L⁻¹ (Yang et al. 2009; Vithanage et al. 2014). A sorbent dose of 1 g L⁻¹ was used for all sorption experiments at an ionic strength of 0.1 M (adjusted by ammonium chloride). The samples were shaken at 100 rpm for 10 selected time intervals (from 0.1 to 96 h) at 25 ± 1 °C. Samples were taken at appointed time intervals and were filtered through Whatman 0.45-μm filters into amber color vials prior to high performance liquid chromatography (HPLC) analysis. The amount of SMT sorbed at any time was calculated from mass balance between initial and final SMT concentrations.

2.3 Data analysis

The SMT concentrations in aqueous solutions (20 μL) were determined using a HPLC system (SCL-10A, Shimadzu, Tokyo, Japan) equipped with an auto-sampler (SIL-10 AD, Shimadzu) and a UV–vis detector (SPD-10A, Shimadzu). A reverse-phase Sunfire C18 column (4.6 mm × 250 mm, Waters, USA) was employed in a column oven (CTO-10AS;

Shimadzu, Japan). The mobile phase A was composed of HPLC grade water and formic acid (99.9:0.1 v/v), while mobile phase B was HPLC grade acetonitrile and formic acid (99.9:0.1 v/v). Mobile phase A of 70 % together with 30 % mobile phase B was then maintained for 20 min. The absorbance was measured at 265 nm.

The sorption kinetics of SMT on unmodified and steam activated biochars were fitted with several kinetic models including pseudo-first order, pseudo-second order, intra-particle diffusion, and Elovich equations, respectively. The pseudo-first order equation which is based on solid capacity (also known as the Lagergren equation) can be expressed as Eq. (1), assuming non-dissociating molecular adsorption (Ho and McKay 1998; Lagergren 1898). Its integrated form can be obtained using the boundary conditions $t = 0$ to $t = t$ and $q_t = 0$ to $q_t = q_t$ (Eq. (2)).

$$\frac{dq}{dt} = k_1(q_e - q_t) \tag{1}$$

$$\log(q_e - q_t) = \log q_e - \frac{k_1 t}{2.303} \tag{2}$$

Where q_t is an amount adsorbed per gram of adsorbent at time t (mg/g), q_e is an amount adsorbed per g of the adsorbent at equilibrium (mg/g); k_1 is Lagergren rate constant (min^{-1}); and t is time (min). The kinetic parameters, correlation coefficients (R^2), and chi square values (χ^2) were obtained from plot of $\log(q_e - q_t)$ against t .

The pseudo-second order equation (Eq. (3)) and its integrated form (Eq. (4)) are expressed as follows (Ho and McKay 1999).

$$\frac{dq}{dt} = k_2(q_e - q_t)^2 \tag{3}$$

$$\frac{t}{q_t} = \frac{1}{k_2 q_e^2} + \frac{t}{q_e} \tag{4}$$

Where q_t is an amount adsorbed per gram of adsorbent at time t (mg/g); q_e is an amount adsorb per g of the adsorbent at equilibrium (mg/g); k_2 is a pseudo second order constant of sorption (mg/g-min); and t is time (min).

The intra-particle diffusion equation describes the sorption as diffusion controlled process that its rate is dependent upon diffusion into the pore system of a spherical particle, which is expressed as Eq. (5) (Wu et al. 2009):

$$q_t = k_{id} t^{1/2} + C \tag{5}$$

Where q_t is mass adsorbed per gram of adsorbent at time t (mg/g); k_{id} is an intra-particle diffusion rate constant (mg/g-min^{0.5}); C is boundary layer effect (mg/g).

The Elovich equation describes chemical sorption on a solid surface without desorption of the products, and hence the rate decreases with time due to an increase in surface

coverage, which can be expressed as Eq. (6) (Ho and McKay 2002; Wu et al. 2009):

$$q_t = \frac{1}{\beta} \ln(\alpha\beta) + \left(\frac{1}{\beta}\right) \ln t \tag{6}$$

Where α is the initial sorption rate (mg/g-min) and β is the sorption constant (unitless).

3 Results and discussion

3.1 Steam activated biochars

Table 1 shows the physico-chemical properties of biochars. Tea waste biochar (TWBC-700) and burcucumber biochar (BBC-700) had contrasting properties (Table 1), reflecting their differences due to the biomass type. Total C content was higher in TWBC-700 (85.1 %) than BBC-700 (69.4 %), while ash content was much lower for TWBC-700 (10.9 %) compared to BBC-700 (43.7 %). This indicated tea waste as a precursor that contain a higher carbonaceous content whereas invasive burcucumber plant had a larger amount of inorganic minerals and non-combustible lignocellulosic structure that remained as ash after pyrolysis. As a result, TWBC-700 (342.2 m² g⁻¹) displayed a notably higher surface area than BBC-700 (2.31 m² g⁻¹), signifying that the properties of

Table 1 Physico-chemical characteristics of unmodified and steam activated biochars

	BBC-700	BBC-700S	TWBC-700	TWBC-700S
Elemental compositions (wt%)				
C	69.4	50.6	85.1	82.4
H	1.31	1.6	1.98	2.06
O	24.5	44.9	8.88	11.6
N	4.61	2.54	3.92	3.89
Molar H/C	0.23	0.39	0.28	0.29
Molar O/C	0.26	0.67	0.08	0.11
Proximate analysis (wt%)				
Moisture	0.33	2.12	4.23	1.40
Mobile matter	13.6	13.2	16.8	18.6
Resident matter	42.4	14.1	68.1	63.2
Ash	43.7	70.7	10.9	16.7
Physical properties				
Surface area (m ² g ⁻¹)	2.31	7.10	342.2	576.1
Pore volume (cm ³ g ⁻¹)	0.008	0.038	0.022	0.109
Pore diameter (nm)	6.780	8.393	1.756	1.998

BBC-700 burcucumber biochar at 700 °C, BBC-700S steam activated burcucumber biochar at 700 °C, TWBC-700 tea waste biochar at 700 °C, TWBC-700S steam activated tea waste biochar at 700 °C

invasive plant-derived biochar may need to be improved for wider potential applications.

Steam activation improved the physical properties and surface chemistry of these biochars. The surface areas of TWBC-700S ($576.1 \text{ m}^2 \text{ g}^{-1}$) and BBC-700S ($7.10 \text{ m}^2 \text{ g}^{-1}$) were significantly increased by 68 and 207 %, respectively. Such increase was probably attributed to the enlarged pore volumes in tea waste biochars (TWBC-700S, $0.109 \text{ cm}^3 \text{ g}^{-1}$; TWBC-700, $0.022 \text{ cm}^3 \text{ g}^{-1}$) and burcucumber biochars (BBC-700S, $0.038 \text{ cm}^3 \text{ g}^{-1}$; BBC-700, $0.008 \text{ cm}^3 \text{ g}^{-1}$) due to steam activation. Steam activation may act as a second-stage partial gasification of biochars which can be effective for creating new porosities and increasing surface area, which in turn significantly increased the sorption capacity (Lima et al. 2010; Rajapaksha et al. 2015).

It was also important to note that, after steam activation, total O contents were increased from 8.88 to 11.6 % (TWBC-700S) and from 24.5 to 44.9 % (BBC-700S), respectively. Simultaneously, total C contents were decreased from 85.1 to 82.4 % and from 69.4 to 50.6 % for TWBC-700S and BBC-700S respectively. The ash contents were increased from 10.9 to 16.7 % for TWBC 700-S and while the increase was 43.7 to 70.7 % for BBC-700S, respectively. These compositional changes reflected that the steam activation could remove the trapped volatile products of pyrolysis and result in partial devolatilization of biochar (Demirbas 2004; Manyà 2012; Chia et al. 2015). Moreover, the molar ratios of O/C and H/C were increased by steam activation, especially for burcucumber biochars due to its lignocellulosic structure. This was in agreement with the suggested reactions of steam activation (Lussier et al. 1998). an initial exchange of oxygen from the water molecule to the carbon surface site creates surface oxide and hydrogen gas, which oxidizes the carbon surface to form surface hydrogen complexes. Thus, steam activation not only enhanced the porosity of biochars but also decreased the hydrophobicity and increased the polarity of the biochar surface, both of which may facilitate the time taken for SMT sorption and pH resilience.

3.2 Enhanced SMT sorption kinetics

As shown in Fig. 1a, the sorption rate of SMT was initially fast, reflecting a large number of vacant sites available for sorption (Guo et al. 2013). followed by a slower sorption process until approaching a plateau gradually. The time taken to reach equilibrium was less for steam activated BCs (~4 h) than non-activated BCs (>24 h). The enhanced sorption kinetics of steam activated biochars could be attributed to the enlargement of pore sizes indicated by the increase in pore diameters as shown in Table 1 (from 1.756 to 1.998 nm in tea waste biochars and from 6.780 to 8.393 nm in burcucumber biochars, respectively). Steam activation was found to be effective for creating new porosities and enlarging diameters of

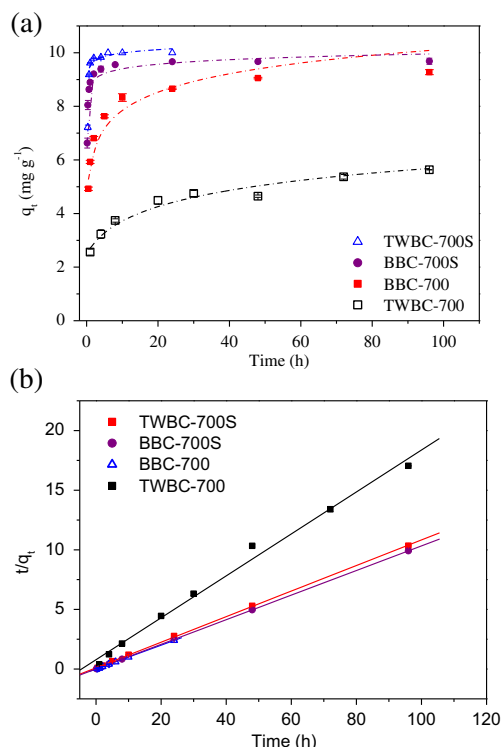


Fig. 1 Sulfamethazine (SMT) sorption kinetics on tea waste biochar at 700 °C (TWBC-700), steam activated tea waste biochar at 700 °C (TWBC-700S), burcucumber biochar at 700 °C (BBC-700), steam activated burcucumber biochar at 700 °C (BBC-700S) at pH 5: **a** sorption data; **b** pseudo-second order kinetic model fitting

smaller pores (Chia et al. 2015; Lima et al. 2010). thereby facilitating the accessibility of internal pores in biochar and accelerating the sorption. This improvement was particularly notable for tea waste biochar (Fig. 1a) which may be due to a majority of its micropores (<2 nm diameter) (Rajapaksha et al. 2014) because water moves much slower in micropores relative to macropores and mesopores. In contrast, burcucumber biochars contained substantial mesopores (2–50 nm diameters) that allowed faster sorption kinetics and the increment by steam activation was less prominent (Rajapaksha et al. 2015). In addition, there was an apparent distinct increase of SMT sorption onto steam activated biochars, of which the equilibrium solid phase concentration followed the order of TWBC-700S > BBC-700S > BBC-700 > TWBC-700.

The best fit kinetic model was selected by considering the calculated correlation coefficient (R^2) and chi-squares (χ^2) values. The estimated kinetic parameters of SMT sorption at pH 5 for all biochars are listed in Table 2. The kinetic data were best described by the pseudo-second order model (Fig. 1b). Besides, the calculated equilibrium sorption (q_{cal}) by pseudo-second order model were comparable to experimentally measured equilibrium sorption (q_{exp}), corroborating that it was the best model to describe the SMT sorption kinetics (Table 2). A good fitting of pseudo-second-order kinetic model suggested that there were abundant sorption sites

Table 2 Fitted parameter values of sorption kinetic models at pH 5

Pseudo-first order model					
	q_{exp} (mg g ⁻¹)	q_{cal} (mg g ⁻¹)	k_1 (min ⁻¹)	R^2	χ^2
BBC-700	9.16	3.00	0.02	0.974	120.9
TWBC-700	5.50	2.32	0.03	0.755	67.7
BBC-700S	9.67	1.53	0.35	0.846	149.9
TWBC-700S	9.95	2.77	1.56	0.850	4.05
Pseudo-second order model					
	q_{exp} (mg g ⁻¹)	q_{cal} (mg g ⁻¹)	k_2 (mg g ⁻¹ min ⁻¹)	R^2	χ^2
BBC-700	9.16	9.33	0.11	0.993	1.41
TWBC-700	5.50	5.71	0.04	0.992	2.38
BBC-700S	9.67	9.69	1.11	1.00	0.06
TWBC-700S	9.95	10.03	1.57	1.00	0.18
Intra-particle diffusion model					
	k_{id} (mg g ⁻¹ min ^{-0.5})	C	R^2	χ^2	
BBC-700	0.82	5.20	0.817	0.67	
TWBC-700	0.37	2.50	0.879	0.15	
BBC-700S	0.92	7.43	0.618	0.57	
TWBC-700S	2.78	6.30	0.686	0.45	
Elovich model					
	α	β	R^2	χ^2	
BBC-700	430.7	0.98	0.969	0.12	
TWBC-700	106.9	0.60	0.973	0.05	
BBC-700S	4.27×10^5	0.68	0.836	0.29	
TWBC-700S	1.42×10^4	0.95	0.688	0.30	

Coefficients of determinations (R^2) and chi-squares values (χ^2)

available on the surface and that the initial concentration of SMT was low compared to the sorption capacity of the biochars (Azizian 2004; Ho 2006; Zhang et al. 2015; Zhu et al. 2015). The pseudo-second order constant of SMT sorption (k_2) derived from the pseudo-second order model showed an increase from 0.04 mg g⁻¹ min⁻¹ in TWBC-700 to 1.57 mg g⁻¹ min⁻¹ in TWBC-700S, and from 0.11 mg g⁻¹ min⁻¹ in BBC-700 to 1.11 mg g⁻¹ min⁻¹ in BBC-700S, respectively. This suggests that SMT sorption by steam activated biochars was 1 to 2 orders of magnitude faster than non-activated biochars. The initial sorption rate at pH 5 was in the order of TWBC-700S > BBC-700S > BBC-700 > TWBC-700. This illustrated the effectiveness of steam activation for enhancing SMT sorption kinetics.

In contrast, pseudo-first order model was not appropriate to describe the experimental data as it showed high χ^2 values and discrepancy between the calculated and measured equilibrium sorption (Table 2). As pseudo-first-order kinetics is most applicable when the initial concentration is high compared to surface coverage (Azizian 2004; Ho 2006; Zhu et al. 2015), the observed non-compliance implies that surface sites on the steam activated biochars are far from saturation. On the other hand, the intra-particle diffusion model and Elovich model

also provided satisfactory fitting to the SMT sorption data on all the biochars studied (Table 2). This may offer indirect evidence of intra-particle diffusion into the polymeric matrix of biochars and decreasing sorption rate with an increase in surface coverage (Ho and McKay 2002; Wu et al. 2009). However, it should be remarked that a conformity of kinetic data to a particular equation (where more than one kinetic models may fit well as shown in this study) does not sufficiently verify the underlying assumptions of rate-limiting steps or sorption mechanisms (Sparks 1999; Benjamin 2002; Tsang et al. 2007; Liu et al. 2008) because the observed sorption kinetics would reflect both transport processes and chemical reactions (Sposito 2004). Nevertheless, the steam activated biochars obviously demonstrated a faster SMT sorption because of increased availability of accessible porous structure with averagely larger pore diameters. This suggests the use of a shorter reaction time or smaller reactor volume that is critical in engineering applications.

3.3 Sorption resilience at varying pH conditions

Since SMT exists as a cationic (SMT⁺), neutral (SMT⁰), anionic (SMT⁻) under different pH conditions (Teixidó et al.

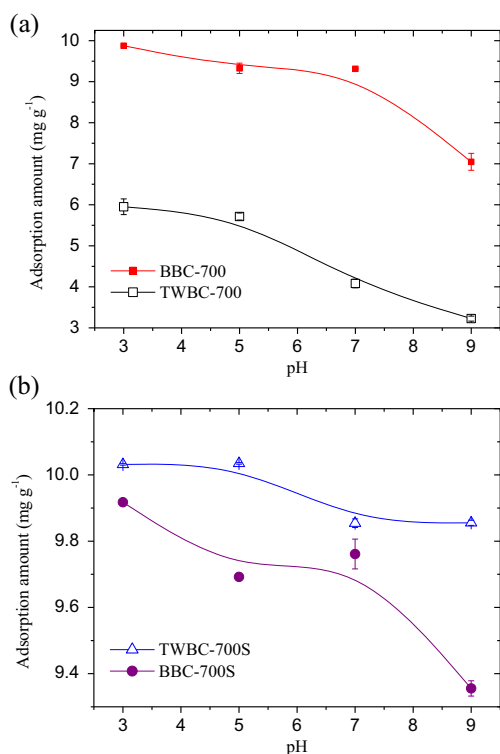


Fig. 2 Equilibrium sorption as a function of pH: **a** non-activated biochars (TWBC-700; BBC-700); **b** steam activated biochars (TWBC-700S; BBC-700S)

2011). It is important to evaluate the sorption resilience of steam activated and non-activated biochars at varying pH values that are environmentally relevant. Figure 2 shows the effect of initial pH values of 3, 5, 7, and 9 on SMT equilibrium sorption, where different species of SMT would dominate over the studied pH range. In view of the two pK_a values of SMT at 2.07 and 7.49 (Qiang and Adams 2004), cationic form (SMT⁺) was prevalent at acidic pH values of 3 and 5. Since the biochars accommodated electron-rich surface that was favorable for cation- π bonding (Ahmad et al. 2014), SMT sorption was less affected by pH change in an acidic range, especially for steam activated biochars that provided much larger surface area (Fig. 2a). However, when the solution pH was increased to 7 and 9, it was seen that the SMT sorption onto non-activated biochars significantly decreased because the neutral (SMT⁰) and anionic (SMT⁻) forms were the dominant species, respectively. In this alkaline pH range, increasing electrostatic repulsion between SMT species and negatively charged biochar surface resulted in the observed suppression on equilibrium sorption by approximately 3 mg g⁻¹ (TWBC-700, from 10 to 7 mg g⁻¹, ~30 % reduction; BBC-700, from 6 to 3 mg g⁻¹, ~50 % reduction).

It is interesting and important to note that steam activated biochars manifested much stronger sorption resilience against pH variation (Fig. 2b). In spite of the same speciation change of SMT across a pH range from 3 to 9, the observed decrease

in equilibrium sorption was only approximately 0.2 mg g⁻¹ on TWBC-700S (from 10.1 to 9.9 mg g⁻¹, ~2 % reduction) and 0.5 mg g⁻¹ on BBC-700S (from 9.9 to 9.5 mg g⁻¹, ~4 % reduction), respectively. Therefore, steam activation of biochars not only enhanced their sorption kinetics and capacities but also rendered SMT sorption onto them more resilient and steady in a pH-variable environment because the enlarged surface area and pore volume mitigated or even offset the effect of unfavorable electrostatic repulsion. These added values of steam activated biochars would make their applications more versatile and reliable in paddy field under seasonal and changeable environmental conditions (Frohne et al. 2015).

4 Conclusions

Antibiotics have been widely applied and led to increasing detection in the environment. The adsorption kinetics of SMT on unmodified and steam activated biochars was well described by pseudo-second order model. It was shown that steam activated biochars were more effective than unmodified biochars in terms of sorption kinetics and capacity as well as resilience against pH variation. Higher surface area and pore volume of steam activated biochars could overcome the unfavorable electrostatic repulsion in alkaline pH range. These kinetic results suggest that steam activation is an effective approach to enhance the performance of biochars for the removal of SMT from water.

Acknowledgments This study was supported by the National Research Foundation of Korea (NRF-2015R1A2A2A11001432).

References

- Ahmad M, Lee SS, Dou X, Mohan D, Sung JK, Yang JE, Ok YS (2012) Effects of pyrolysis temperature on soybean stover- and peanut shell-derived biochar properties and TCE adsorption in water. *Bioresour Technol* 118:536–544
- Ahmad M, Rajapaksha AU, Lim JE, Zhang M, Bolan N, Mohan D, Vithanage M, Lee SS, Ok YS (2014) Biochar as a sorbent for contaminant management in soil and water: a review. *Chemosphere* 99: 19–23
- Aust MO, Thiele-Bruhn S, Seeger J, Godlinski F, Meissner R, Leinweber P (2010) Sulfonamides leach from sandy loam soils under common agricultural practice. *Water Air Soil Pollut* 211:143–156
- Azizian S (2004) Kinetic models of sorption: a theoretical analysis. *J Colloid Interface Sci* 276:47–52
- Benjamin MM (2002) Adsorption reactions. *Water chemistry*. McGraw-Hill, New York, pp 550–627
- Boxall ABA, Fogg LA, Blackwell PA, Blackwell P, Kay P, Pemberton EJ, Croxford A (2004) Veterinary medicines in the environment. *Rev Environ Contam Toxicol*, Springer, New York, pp 1–91
- Chia CH, Downie A, Munroe P (2015) Characteristics of biochar: physical and structural properties. In: Lehmann J, Joseph S (eds) *Biochar for environmental management*. Earthscan, London, pp 89–111

- Demirbas A (2004) Effects of temperature and particle size on bio-char yield from pyrolysis of agricultural residues. *J Anal Appl Pyrolysis* 72:243–248
- Frohne T, Diaz-Bone RA, Du Laing G, Rinklebe J (2015) Impact of systematic change of redox potential on the leaching of Ba, Cr, Sr, and V from a riverine soil into water. *J Soils Sediments* 15:623–633
- Guo X, Yang C, Dang Z, Zhang Q, Li Y, Meng Q (2013) Sorption thermodynamics and kinetics properties of tylosin and sulfamethazine on goethite. *Chem Eng J* 223:59–67
- Haller MY, Müller SR, McArdeell CS, Alder AC, Suter MJF (2002) Quantification of veterinary antibiotics (sulfonamides and trimethoprim) in animal manure by liquid chromatography–mass spectrometry. *J Chromatogr A* 952:111–120
- Hamscher G, Szczesny S, Höper H, Nau H (2002) Determination of persistent tetracycline residues in soil fertilized with liquid manure by high-performance liquid chromatography with electrospray ionization tandem mass spectrometry. *Anal Chem* 74:1509–1518
- Ho YS (2006) Review of second-order models for adsorption systems. *J Hazard Mater* 136:681–689
- Ho YS, McKay G (1998) Sorption of dye from aqueous solution by peat. *Chem Eng J* 70:115–124
- Ho YS, McKay G (1999) Pseudo-second order model for sorption processes. *Process Biochem* 34:451–465
- Ho YS, McKay G (2002) Application of kinetic models to the sorption of copper (II) on to peat. *Adsorpt Sci Technol* 20:797–815
- Kim KR, Owens G, Kwon SI, So KH, Lee DB, Ok YS (2011) Occurrence and environmental fate of veterinary antibiotics in the terrestrial environment. *Water Air Soil Pollut* 214:163–174
- Lagergren S (1898) Zurtheorie der sogenannten adsorption gelosterstoffe. *Kungliga Svenska Vetenskapsakademiens Handlingar* 24:1–39
- Lehmann J, Joseph S (2009) *Biochar for environmental management: science and technology*. Earthscan, London
- Lim JE, Rajapaksha AU, Jeong SH, Kim SC, Kim KH, Lee SS, Ok YS (2014) Monitoring of selected veterinary antibiotics in animal carcass disposal site and adjacent agricultural soil. *J Appl Biol Chem* 57:189–196
- Lima IM, Boateng AA, Klasson KT (2010) Physicochemical and adsorptive properties of fast-pyrolysis bio-chars and their steam activated counterparts. *J Chem Technol Biotechnol* 85:1515–1521
- Liu MY, Tsang DCW, Hu J, Ng KTW, Liu T, Lo IMC (2008) Adsorption of methylene blue and phenol by wood waste derived activated carbon. *J Environ Eng* 134:338–345
- Lussler MG, Zhang Z, Miller DJ (1998) Characterizing rate inhibition in steam/hydrogen gasification via analysis of adsorbed hydrogen. *Carbon* 36:1361–1369
- Manyà JJ (2012) Pyrolysis for biochar purposes: a review to establish current knowledge gaps and research needs. *Environ Sci Technol* 46:7939–7954
- Margalida A, Bogliani G, Bowden CGR, Donázar JA, Genero F, Gilbert M, Karesh WB, Kock R, Lubroth J, Manteca X, Naidoo V, Neimanis A, Sánchez-Zapata JA, Taggart MA, Vaarten J, Yon L, Kuiken T, Green RE (2014) One health approach to use of veterinary pharmaceuticals. *Science* 346:1296–1298
- Mohan D, Sarswat A, Ok YS, Pittman CU Jr (2014) Organic and inorganic contaminants removal from water with biochar: a renewable, low cost and sustainable adsorbent—a critical review. *Bioresour Technol* 160:191–202
- Novak JM, Lima I, Xing B, Gaskin JW, Steiner C, Das KC, Ahmedna M, Rehrah D, Watts DW, Busscher WJ, Harry S (2009) Characterization of designer biochar produced at different temperatures and their effects on a loamy sand. *Ann Environ Sci* 3:195–206
- Ok YS, Kim SC, Kim KR, Lee SS, Moon DH, Lim KJ, Sung JK, Hur SO, Yang JE (2011) Monitoring of selected veterinary antibiotics in environmental compartments near a composting facility in Gangwon Province, Korea. *Environ Monit Assess* 174:693–701
- Qiang Z, Adams C (2004) Potentiometric determination of acid dissociation constants (pKa) for human and veterinary antibiotics. *Water Res* 38:2874–2890
- Rajapaksha AU, Vithanage M, Zhang M, Ahmad M, Mohan D, Chang SX, Ok YS (2014) Pyrolysis condition affected sulfamethazine sorption by tea waste biochars. *Bioresour Technol* 166:303–308
- Rajapaksha AU, Vithanage M, Ahmad M, Seo DC, Cho JS, Lee SE, Lee SS, Ok YS (2015) Enhanced sulfamethazine removal by steam-activated invasive plant-derived biochar. *J Hazard Mater* 290:43–50
- Rinklebe J, Shaheen SM, Frohne T (2015) Amendment of biochar reduces the release of toxic elements under dynamic redox conditions in a contaminated floodplain soil. *Chemosphere* 142:41–47
- Sparks DL (1999) *Soil physical chemistry*, 2nd edn. CRC Press, New York
- Sposito G (2004) *The surface chemistry of natural particles*. Oxford University Press, New York
- Teixidó M, Pignatello JJ, Beltrán JL, Granados M, Peccia J (2011) Speciation of the ionizable antibiotic sulfamethazine on black carbon (biochar). *Environ Sci Technol* 45:10020–10027
- Thiele-Bruhn S (2003) Pharmaceutical antibiotic compounds in soils—a review. *J Plant Nutr Soil Sci* 166:145–167
- Tsang DCW, Yip ACK (2014) Comparing chemical-enhanced washing and waste-based stabilisation approach for soil remediation. *J Soils Sediments* 14:936–947
- Tsang DCW, Hu J, Liu M, Zhang W, Lai KCK, Lo IMC (2007) Activated carbon produced from waste wood pallets: adsorption of three classes of dyes. *Water Air Soil Pollut* 184:141–155
- Uchimiya M, Chang S, Klasson KT (2011) Screening biochars for heavy metal retention in soil: role of oxygen functional groups. *J Hazard Mater* 190:432–441
- Vithanage M, Rajapaksha AU, Tang X, Thiele-Bruhn S, Kim KH, Lee SE, Ok YS (2014) Sorption and transport of sulfamethazine in agricultural soils amended with invasive-plant-derived-biochar. *J Environ Manag* 141:95–103
- Wang S, Gao B, Zimmerman AR, Li Y, Ma L, Harris WG, Migliaccio KW (2015) Removal of arsenic by magnetic biochar prepared from pinewood and natural hematite. *Bioresour Technol* 175:391–395
- Wu FC, Tseng RL, Juang RS (2009) Characteristics of Elovich equation used for the analysis of adsorption kinetics in dye-chitosan systems. *Chem Eng J* 150:366–373
- Yang JF, Ying GG, Yang LH, Zhao JL, Liu F, Tao R, Yu ZQ (2009) Degradation behavior of sulfadiazine in soils under different conditions. *J Environ Sci Health Part B* 44:241–248
- Zhang W, Zheng J, Zheng P, Tsang DCW, Qiu R (2015) Sludge-derived biochar for arsenic(III) immobilization: effects of solution chemistry on sorption behavior. *J Environ Qual* 44:1119–1126
- Zhu X, Tsang DCW, Chen F, Li S, Yang X (2015) Ciprofloxacin adsorption on graphene and granular activated carbon: kinetics, isotherms, and effects of solution chemistry. *Environ Technol* 36:3094–3102